IEEE Access
Multidisciplinary | Rapid Review | Open Access Journal

Received April 7, 2019, accepted May 23, 2019, date of publication June 5, 2019, date of current version June 21, 2019.

Digital Object Identifier 10.1109/ACCESS.2019.2921005

Noncontact Thickness Measurement of Cu Film on Silicon Wafer Using Magnetic Resonance Coupling for Stress Free Polishing Application

ZILIAN QU[1], WENSONG WANG[2], (Member, IEEE), SHUHUI YANG[3], (Member, IEEE), QUQIN SUN[2], ZHONGYUAN FANG[2], AND YUANJIN ZHENG[2], (Senior Member, IEEE)

[1]Beijing Information Technology College, Beijing 100015, China
[2]School of Electrical and Electronic Engineering, Nanyang Technological University, Singapore 639798
[3]Department of Communication Engineering, Communication University of China, Beijing 100024, China

Corresponding author: Wensong Wang (uscnuaa@gmail.com; wangws@ntu.edu.sg)

This work was conducted in the SMRT-NTU Smart Urban Rail Corporate Laboratory supported in part by the National Research Foundation (NRF), in part by the SMRT, and in part by the Nanyang Technological University, under the Corp Lab@University Scheme.

ABSTRACT A novel noncontact measurement method based on double-coil sensor is proposed for determining the thickness of copper (Cu) film on the silicon wafer in the process of stress free polishing (SFP). The double-coil sensor consists of two identical coaxial eddy current coils and corresponding auxiliary circuits, where the two coils are excited with the same sinusoidal signal and interact through the magnetic resonance coupling. The induced currents are produced in the Cu film through the electromagnetic coupling between double coils. The interaction equivalent circuit model of Cu film and two coils of double-coil sensor is discussed and the coil design and its lumped parameter extraction are analyzed. The linear relationship between the inductance difference of two coils and lift-off distance change (LODC) is formed and analyzed. By simulating the Cu film with different thicknesses sandwiched between two coils, the distribution and intensity of the magnetic field are presented. The slope of the relationship line between the inductance difference and the LODC is termed as SOR. Dependent on the LODC, the relationship between SOR and thickness of Cu film is extracted. Finally, the double-coil sensor is fabricated and the experiment is implemented. Different specimens with the thickness ranges from 100 to 500 nm are prepared and measured, where the measured maximum relative error is 4.7% and standard errors are between 2 and 13 nm. The experimental results demonstrate that the proposed measurement method is feasible and can confirm the thickness of Cu film on the silicon wafer. It is not only insensitive to the LODC but also can measure the thickness of less than 1 μm for Cu film on the silicon wafer.

INDEX TERMS Double-coil sensor, magnetic resonance coupling, Cu film on the silicon wafer, stress free polishing, equivalent circuit model.

I. INTRODUCTION

Chemical mechanical planarization (CMP) is a key technique in the current semiconductor manufacturing process [1]. The CMP is a polishing process and utilizes the mechanical polishing with the chemical slurry formulation for removing the unwanted conductive and dielectric materials on the silicon wafer. A typical CMP machine contains a rotation wafer chuck and an extremely flat polish plate which is covered by a polish pad. In the process of the polishing, the silicon wafer is mounted upside-down in the chuck and rotated with it. The downforce from the chuck pushes the silicon wafer against the polishing pad and the material on the silicon wafer is removed by the friction force combining with the slurry. In the Cu damascene process [2], the copper CMP (Cu-CMP) technology is adopted to remove the excess Cu material. Then, only the Cu material in the grooves of silicon basement is retained and the Cu interconnect line in semiconductor devices is finally formed.

With the development of semiconductor devices in recent years, the low-κ dielectric barrier materials have been widely employed to overcome the time delay in the semiconductor

The associate editor coordinating the review of this manuscript and approving it for publication was Bora Onat.

circuit [3]. Meanwhile, the line-width of Cu interconnects has fallen to less than 20 nm in the very large scale integrated circuit, which makes the chip more powerful and smaller. Under the situation, the strength of material on the silicon wafer decreases and the traditional CMP technique would give rise to damages to the Cu interconnects because of the high downforce from the polishing chuck. To overcome the problem, two-step stress free polishing (SFP) technology has been studied in recent years [4], [5]. For the first step, the traditional CMP process is applied to remove a large portion of the Cu film on the silicon wafer till the thickness of Cu film is reduced to about 200 nm $\sim$ 300 nm. For the second step, the electrochemical polishing approach is shifted on the silicon wafer to remove the remaining Cu structures and avoid damaging the soft material. In the SFP, the electrolyte sprays onto the surface of the silicon wafer and then the excess Cu layer is removed by the electrochemical corrosion without downforce on the silicon wafer. The SFP can avoid the damage of Cu interconnects and other soft materials on the silicon wafer.

In the SFP, the amount of the electrolyte sprayed on Cu film determines the removing rate of Cu film, and the uniform removing rate can improve the accuracy of the circuits. The thickness distribution of the Cu film provides the feedback information which can control the modules for adjusting the amount of electrolyte spray on the Cu film surface, and avoid the over etching [6]–[9]. In order to measure the thickness of Cu film, various methods have been investigated in the past several years, such as optical reflectivity method [10], four-point probe (4PP) method [11] and eddy current technique [12]. In the semiconductor industry, the 4PP method is the most common used method for determining the thickness of the conductive film, and needs the probe to contact the surface of the sample. However, for the SFP, the thickness measurement of Cu film needs to be noncontact and nondestructive. Only the eddy current technique could meet the requirements with features of high efficiency, high sensitivity, especially nondestructive and noncontact ability [13]–[16].

When applying the traditional eddy current method with only one coil to detect the thickness of Cu film on the silicon wafer, the distance between the sensor coil and Cu film, known as lift-off distance (LOD), needs to be kept unchanged. The distance change posts a strong negative effect on accuracy and repetitiveness of the measurement. The inductance of the coil is not only sensitive to the thickness variation, but also the LOD changes (LODCs). The inescapable LODCs originate from the mechanical vibration and the runout position error due to the silicon wafer chuck rotation, as shown in Fig. 1.

To minimize the LODC effect for measuring the thickness of Cu film by using the eddy current technique, two methods have been explored. One is the multi-frequency eddy current (MEC) method [17]–[19] and the other is the pulsed eddy current (PEC) method [20]. For the MEC method, the eddy current coil is excited by a sweep frequency signal,

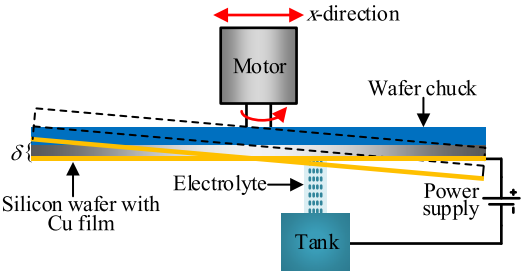

FIGURE 1. A model for the process of stress free polishing.

the real and imaginary parts of the impedance of the coil are collected and the certain electrical parameter is extracted for reflecting the thickness of conductive film immune to the LODCs. In [21], it demonstrated that the peak frequency of the imaginary part of the inductance change is inversely proportional to the thickness of the conductive film, and the peak frequency is relatively unaffected by the LODCs. For the PEC method [22]–[24], two coils are adopted and the pulsed current signal is fed into the excitation coil. Then, the signal in the pickup coil is analyzed. The most popular feature to be used for minimizing the LODC effect is called as lift-off point of intersection (LOI), which can be observed in the pickup signal in the time domain with the LOD varying. Both MEC and PEC methods have the capacity to diminish the LODC effect on the accuracy of conductive film thickness, however, they need complex frequency analysis and high-quality hardware for guaranteeing the signal processing efficiency. These characteristics lead to time-consuming as well as high economic cost. Therefore, these factors limited their utilization in the thickness measurement of Cu film in the SFP. Also, it is challenging to obtain the accurate thickness of Cu film remaining on the silicon wafer during the SFP.

In the previous work for the thickness measurement of Cu film [25], the parameters such as the diameter/height ratio and working frequency of eddy current coil are optimized for increasing the uniformity of electromagnetic field along the axis of the primary coil, which can reduce the LODC influence. However, it is hard to uniform the electromagnetic field along the axial completely. When the LOD varies, the magnetic coupling coefficient between the coil and induced eddy current in the Cu film is changed. The change of the impedance of eddy current coil can reflect simultaneously the information about thickness variation of Cu film and LODC.

In this paper, a noncontact measurement method based on double-coil sensor is proposed, which contains two eddy current coils and auxiliary circuits for measuring the thickness of Cu film on the silicon wafer. Firstly, it is presented for the theoretical analysis of eddy current technique using two identical coaxial coils to confirm the thickness of Cu film. Secondly, the double-coil sensor sandwiching the Cu film is analyzed and its interaction equivalent circuit model (ECM) is illustrated. Meantime, the coil design and corresponding lumped parameter extraction are introduced, and the electromagnetic field simulations are also conducted under different Cu film thicknesses to observe the distribution and intensity

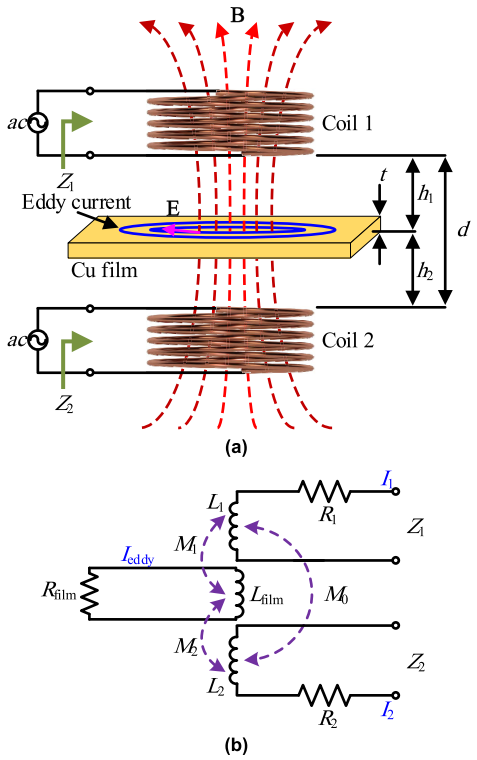

FIGURE 2. (a) Two coaxial coils and Cu film, and (b) ECM.

of the magnetic field. Then, the relationship between the SOR and the thickness of Cu film is extracted. Finally, the experiment setup is established and the thickness distribution of Cu film on the silicon wafer is measured. The measured relative error and standard error are evaluated for prepared specimens. Also, the measurement procedure is summarized. The proposed method can measure the thickness of less than 1 μm for Cu film on the silicon wafer, and lower the negative effect of LODC with high speed and low cost.

II. THEORETICAL ANALYSIS

The proposed noncontact measurement method based on double-coil sensor mainly utilizes the magnetic resonance coupling of two coaxial coils. Considering a coil positioned on a Cu film sample as shown in Fig. 2(a), when the time-varying current is fed into the coil, and the time-varying magnetic field $\mathbf{B}(\mathbf{r})$ is generated and calculated by using the Bio-Savart Law

$$\mathbf{B}(\mathbf{r}) = \frac{\mu_0 NI}{4\pi} \oint_C \frac{dl' \times (\mathbf{r} - \mathbf{r}')}{(\mathbf{r} - \mathbf{r}')^3} \tag{1}$$

where C, I, μ_0, N and dl' are the whole current path, the magnitude of the current flowing through the coil, the permeability of free space, number of turns of the coil, and differential coil element, respectively. $\mathbf{r}$ and $\boldsymbol{r}'$ are the position vectors of the observation point and dl', respectively. In the presence of the time-varying $\mathbf{B}(\mathbf{r})$, the electromotive force (i.e., voltage) is produced within the Cu film. The magnitude of the induced voltage is proportional to the rate of change of the $\mathbf{B}(\mathbf{r})$ in the given area, and its direction is defined by Lenz's law. The phenomenon can be explained by the differential form of Faraday's law of induction, i.e., Maxwell-Faraday equation

$$\nabla \times \mathbf{E}(\mathbf{r}) = -\frac{\partial \mathbf{B}(\mathbf{r})}{\partial t'} \tag{2}$$

where $\mathbf{E}(\mathbf{r})$ is the time-varying electric field, and t' is the time variable. Due to a driven voltage, the eddy current is formed within the conductor and in plane perpendicular to the $\mathbf{B}(\mathbf{r})$. The eddy current density $\mathbf{J}(\mathbf{r})$ in the given area is computed through the Ohm's law

$$\mathbf{J}(\mathbf{r}) = \sigma \mathbf{E}(\mathbf{r}) \tag{3}$$

where σ is the electrical conductivity of the conductive material. The eddy current loop will generate a magnetic field opposing the magnetic flux change which induces the eddy current by the two coils. In order to measure the thickness of Cu film, the penetrating depth of the induced eddy current must be larger than the thickness of Cu film. The penetrating depth can be described by the skin depth in the conductive material, which is defined as the depth below the surface of the Cu film where the current density has fallen to $1/e$ of the surface current density. The skin depth is expressed by

$$\delta = \frac{1}{\sqrt{\pi f \sigma \mu_r \mu_0}} \tag{4}$$

where f is the frequency of excitation signal in the coil, μ_r is the relative permeability, and μ_0 is the permeability in free space. Usually, the f is from 0.5 MHz to 5 MHz in the measurement, and the corresponding skin depth δ is from 92.2 μm to 11.9 μm. The thickness of Cu film, t, is from 50 nm to 500 nm, thereby t is largely less than δ.

The eddy current loop induced in the Cu film can be simplified and equivalent to a resistor R_{eddy} and an inductor L_{eddy} in series, which couples with the two coils as a transformer model. Each coil can be simplified as a resistor R_1/R_2 and an inductor L_1/L_2 in series. The ECM of two coils sandwiching the Cu film is shown in Fig. 2(b). The coil 1 and coil 2 interact with the eddy current loop through the mutual inductance M_1 and M_2. When the distance between coil 1 and coil 2, d, is several mm, the magnetic field between them can be considered as the uniform, and the diameter of the induced eddy current is unchanged. When the Cu film is sandwiched between them, the mutual inductance between coil 1 and coil 2, M_0, can be kept unchanged.

Based on the Kirchhoff voltage law [26]–[29], the input impedances of coil 1 and coil 2 are respectively written as

$$Z_1 = R_1 + j\omega [L_1 - M_1 + M_0] \tag{5}$$
$$Z_2 = R_2 + j\omega [L_2 - M_2 + M_0] \tag{6}$$

where $\omega = 2\pi f$, $R_1 = R_2$, $L_1 = L_2$. From Eq. (5)–Eq. (6),

$$Z_2 - Z_1 = j\omega [M_1 - M_2] \tag{7}$$

Also,

$$M_1 = k_1\sqrt{L_1 L_{film}} \tag{8}$$

$$M_2 = k_2\sqrt{L_2 L_{film}} \tag{9}$$

where k_1 and k_2 are mutual coefficients, which are related to the distance between the coil and Cu film. L_{film} is the equivalent inductance of the eddy current loop in the Cu film. When the distance becomes smaller, the mutual coefficient is larger. Substituting Eqs. (5) and (6) into Eq. (7),

$$Z_2 - Z_1 = j\omega\left[k_1\sqrt{L_1 L_{film}} - k_2\sqrt{L_2 L_{film}}\right] \tag{10}$$

Since L_1 is equal to L_2,

$$Z_2 - Z_1 = j\omega(k_1 - k_2)\sqrt{L_1 L_{film}} \tag{11}$$

According to the definition of the inductance which is equal to the ratio of magnetic flux to current, the L_{film} is written as

$$L_{film} = tL'_{film} = \frac{t\Phi}{\int\limits_S \mathbf{J}(\mathbf{r})\, ds} \tag{12}$$

where L'_{film} is the equivalent inductance per unit height, S is the given area which the magnetic field passes through, t is the thickness of Cu film, Φ is magnetic flux density. When the double-coil sensor is moving, Φ is kept unchanged. Substituting Eq. (12) into Eq. (11),

$$Z_2 - Z_1 = j\omega(k_1 - k_2)\sqrt{L_1 \frac{t\Phi}{\int\limits_S \mathbf{J}(\mathbf{r})\, ds}} \tag{13}$$

Inductance different is defined as

$$\Delta L = (k_1 - k_2)\sqrt{L_1 \frac{t\Phi}{\int\limits_S \mathbf{J}(\mathbf{r})\, ds}} \tag{14}$$

When k_1 is equal to k_2, Cu film is located at the center of two coils, and the inductance different is zero. Considering the distance between both coils is much shorter than the diameter of each coil, the mutual coefficient is approximately linear to the distance. k_1 and k_2 can be written as

$$k_1 = ph_1 \tag{15}$$

$$k_2 = ph_2 \tag{16}$$

where p is mutual coefficient factor. h_1 and h_2 are the distance between the coil 1 and Cu film and the distance between the coil 2 and Cu film, respectively.

$$\Delta L = (h_1 - h_2)\, p\sqrt{L_1 \frac{t\Phi}{\int_S \mathbf{J}(\mathbf{r})\, ds}} = \Delta h \cdot p\sqrt{L_1 \frac{t\Phi}{\int_S \mathbf{J}(\mathbf{r})\, ds}} \tag{17}$$

where Δh is the LODC and equal to h_1 - h_2. When the coil 1 or coil 2 is close to Cu film, the slope of inductance difference will be affected by $p\sqrt{L_1 \frac{t\Phi}{\int_S \mathbf{J}(\mathbf{r})ds}}$. The change of inductance difference indicates the thickness change of the Cu film. As the thickness of Cu film increases, the inductance difference also increases. The LODC becomes an independent parameter that has no relationship with the thickness of Cu film, which will not affect the accuracy of the thickness during the measurement.

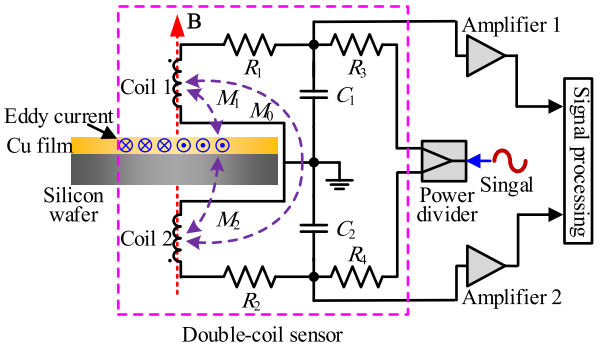

FIGURE 3. Proposed noncontact measurement method based on double-coil sensor for confirming the thickness of Cu film on silicon wafer.

III. NONCONTACT MEASUREMENT METHOD BASED ON DOUBLE-COIL SENSOR

To obtain accuracy information of the thickness of Cu film on the silicon wafer under different LODCs in the SFP, a noncontact measurement method based on double-coil sensor is analyzed, designed and discussed.

A. DOUBLE-COIL SENSOR

As shown in Fig. 3, it is the noncontact measurement method based on double-coil sensor for confirming the thickness of Cu film on the silicon wafer. Two coaxial air-core coils are key parts of the sensor, which are with same turns, material, working frequency, and uniform electrical parameters. They are separately located at both sides of the silicon wafer. In order to convert the inductance changes of two coils to the output voltage for picking up and processing, the bridge circuit is adopted to convert the inductance variation of the coil to the voltages change. In the SFP machine, the silicon wafer chuck is made of plastic polymer material where the resistance is high enough to damp the generation of eddy current in it. Thus, the electromagnetic field generated in free space by coils can pass through the wafer chuck without any loss.

The permeability of Cu film is constant and the skin depth of eddy current is only related to the working frequency of the coil. Comparing with the thickness of Cu film in the SFP ranging from 100 nm to 500 nm, the attenuation of eddy current along the depth in the Cu film can be ignored and the eddy current can be considered as simplified current loops with the uniform current density.

Fig. 4 shows the interaction ECM of the Cu film and two coils of the double-coil sensor, where it includes three mutual inductances, M_0, M_1, and M_2. The coils and Cu film are magnetically coupled with each other through the three mutual

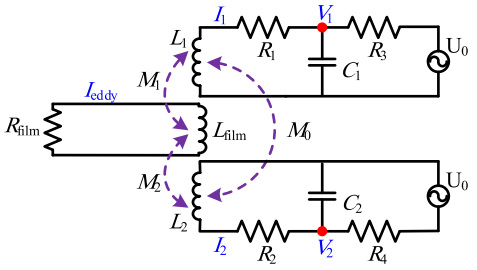

FIGURE 4. Interaction ECM of Cu film and two coils of double-coil sensor.

inductances [30]. The capacitors C_1 and C_2 are parallelly connected with the two coils, respectively. When the bridge circuit is operating at the frequency of ω, the voltages probed at the coil 1 and coil 2 can be respectively expressed as follows

$$V_1 = U_0 \frac{Z_{L1C1}}{R_3 + Z_{L1C1}} \tag{18}$$

$$V_2 = U_0 \frac{Z_{L2C2}}{R_4 + Z_{L2C2}} \tag{19}$$

where

$$Z_{L1C1} = \frac{(R_1 + j\omega L_1')(1/j\omega C_1)}{R_1 + j\omega L_1' + (1/j\omega C_1)} \tag{20}$$

$$Z_{L2C2} = \frac{(R_2 + j\omega L_2')(1/j\omega C_2)}{R_2 + j\omega L_2' + (1/j\omega C_2)} \tag{21}$$

where L_1' and L_2' are the equivalent inductances of the coil 1 and coil 2, respectively, which can be written as

$$L_1' = L_1 - M_1 + M_0 \tag{22}$$

$$L_2' = L_2 - M_2 + M_0 \tag{23}$$

By testing the voltages at the coil 1 and coil 2, the equivalent inductances can be analyzed and extracted.

B. COIL DESIGN AND LUMPED PARAMETER EXTRACTION

This paper focuses on a planar coil design used in the proposed measurement method. The physical parameters such as inner and outer radii and distribution of turns are swept for optimization using the traditional method. The planar coil is specifically optimized to reduce the stray magnetic fields and finalized with the outer radius of 2.5 mm and inner radius of 0.875 mm with 8 turns. Lumped parameters of the coil are extracted accurately to ensure the optimum series capacitor for quantifying the intensity of the magnetic field. The prototyped coil is fabricated on the printed circuit board shown in Fig. 5(a) and measured by an Impedance Analyzer (Agilent 4294A). The common lumped parameter model of a coil consists of an inductor with the inductance of L_1, and a resistor with the resistance of R_1, connected in series, shown in Fig. 5(a). The measured data of the resistance and inductance are shown in Fig. 5(b).

R_1 is calculated through the MATLAB tool according to the recursive optimization method and plotted in Fig. 5(b), wherein the measured direct-current resistance is 0.28 Ω.

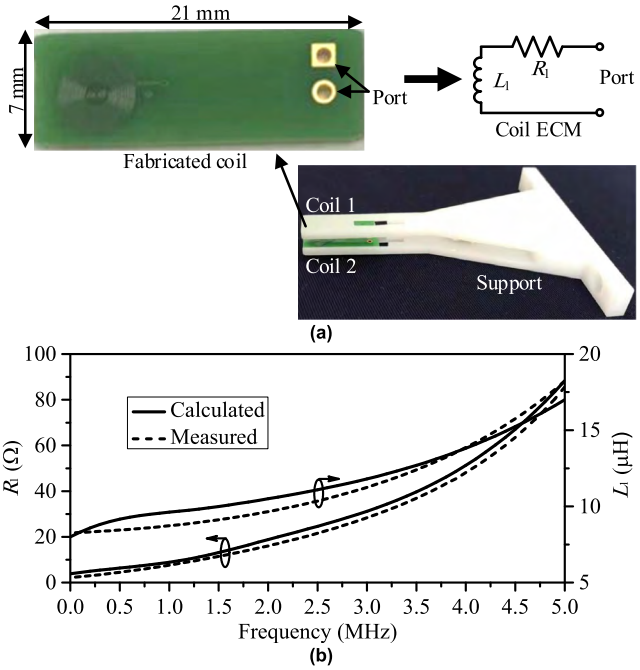

FIGURE 5. (a) Coil prototype and ECM, and (b) coil resistance and inductance with frequency varying.

Also, the inductance L_1 of the coil is calculated using FEM simulation and shown in Fig. 5(b). Both of them are consistent with the measured results for the coil. It is seen that the resistance and inductance at 0.5 MHz are 4.52 Ω and 7.23 μH, respectively, where the measured quality factor is about 11.7.

The capacitor connected to both terminals in parallel is adopted to tune the resonance frequency of the coil and the capacitance is set according to

$$C_1 = \frac{1}{(2\pi f_0)^2 L_1} \tag{24}$$

where f_0 is the working frequency. When the f_0 is at 0.5 MHz, the C_1 is calculated to be 9.46 nF by applying Eq. 24.

C. ELECTROMAGNETIC FIELD SIMULATION

To analyze the distribution of eddy current density in the thin Cu film, the simulation model with two coils is set up by using Ansys Maxwell simulation tool as shown in Fig. 6. Each coil is the planar circular spiral winding with 8 turns and the inner and outer diameters are 2 mm and 5 mm, respectively. The cross-section of the coil wire is within a square of 0.1 mm × 0.1 mm and the distance between two coils is 1.5 mm. Then, a Cu film with different LODs is located between two coils for simulations. Fig. 6 shows the simulation model of two coils and Cu film. The average radius of each coil is indicated as R, which is equal to $(r_1 + r_2)/2$. The distance between the two coils is indicated as d. The Cu film is located at the middle position between coil 1 and coil 2, and h is $d/2$, where the maximum LODC is Δh. When the Cu film is moving in the

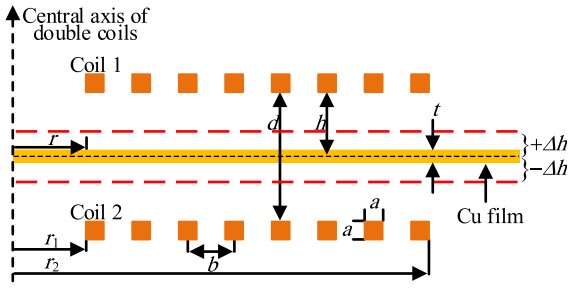

FIGURE 6. Simulation model of two coils and Cu film.

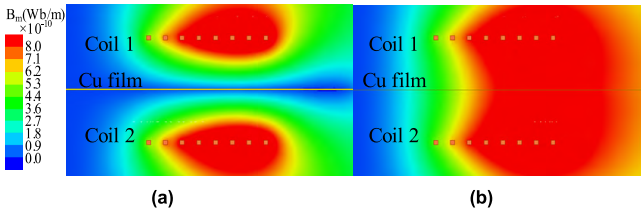

FIGURE 7. Magnetic flux density distribution for (a) Cu film thickness of 50 μm, and (b) Cu film thickness of 1 μm.

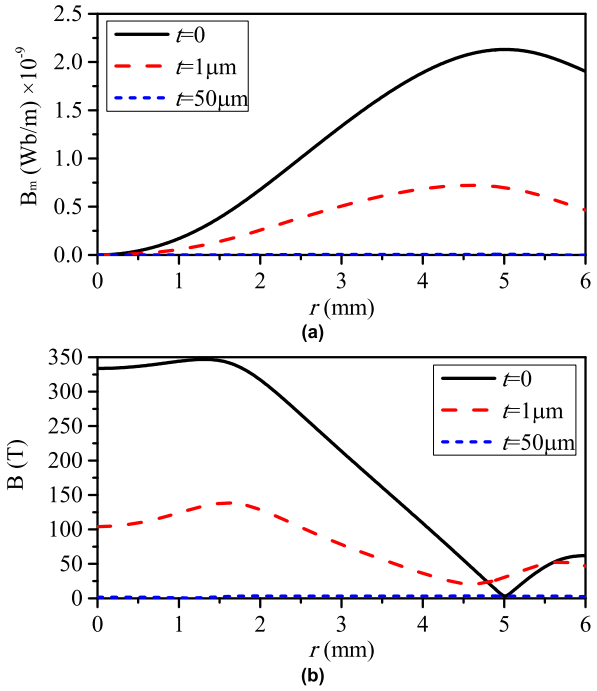

FIGURE 8. Magnetic field intensity along the middle line of Cu film with different thicknesses. (a) Magnetic flux intensity, and (b) magnetic field.

range of Δh, the inductance of each coil is changed and the difference of them is calculated.

The thickness of Cu film is set as 50 μm and 1 μm, respectively, and the LOD between the Cu film and the coil 1 is 0.75 mm. The excitation signal is with the frequency of 0.5 MHz and the amplitude of 1 A. The distributions of the magnetic field under different Cu film thicknesses are simulated and shown in Figs. 7(a) and (b).

As shown in Fig. 7(a), when the thickness of Cu film is 50 μm, which is thicker than the skin depth in the Cu film, the magnetic field cannot penetrate the Cu film where the film behaves like an electromagnetic mirror. The change of LOD can cause the inductance variation of the coil. When the thickness of Cu film is set as 1 μm, which is thinner than the skin depth, the magnetic field will penetrate the Cu film as shown in Fig. 7(b). The intensity of the electromagnetic field in the middle of the Cu film is presented in Fig. 8. Compared with the case without Cu film, the intensity of electromagnetic field is weakened by the opposite electromagnetic field from the Cu film. The changes of the thickness of Cu film and the LOD jointly contribute to the inductance change of the coil and the thickness of Cu film plays a major role.

D. CU FILM THICKNESS EXTRACTION

In the model as shown in Fig. 6, R is 1.75 mm and the d is 1.5 mm. A Cu film with $t = 0.5\mu$m is placed in the middle position between two coils ($h = 0.75$ mm) and the Δh is set to 0.2 mm. When the position of Cu film changes from $-\Delta h$ to $+\Delta h$, the inductance of each coil will be changed. The simulation results of the inductances of two coils are shown in Fig. 9. It shows that when the position of Cu film is moving from 0 to 0.2 mm, the inductance of coil 2 increases while for coil 1 it decreases. When the Cu film is at the position of $h = d/2(\Delta h = 0)$, the inductances of two coils are equal and thus the inductance difference is zero, while at the positions of $+\Delta h$ and $-\Delta h$, the inductance difference will increase to the maximum value.

When d varies from 1.5 mm, 2.5 mm to 3.5 mm, the inductance difference of two coils under different LODCs are analyzed and the evaluated results are presented in Fig. 10. It indicates that the distance between the two coils plays an effect. When the d exceeds a certain value, the linearity degree of the inductance difference will decrease. In order to evaluate the inductance changes under different thicknesses of Cu film, the thickness of Cu film is set from 5 μm, 40 μm to 50 μm, and the LOD between coil 1 and Cu film is from 0.55 mm to 0.95 mm with the step of 0.05 mm. The relationship between the inductances of two coils and the LODCs is shown in Fig. 11.

From Fig. 11, with the increase of the LODC, the inductance of coil 2 increases, while the inductance of coil 1 decreases. When the Cu film is at the middle position between coil 1 and coil 2, the mutual inductance between each coil and the eddy current loop in the Cu film is equal to each other. The cross point between the two inductances corresponds to the middle positon between the two coils. As the thickness of Cu film decreases, the intersection slope of both inductances for coil 2 and coil 1 decreases.

The inductance differences of the coil 2 and coil 1 under different thicknesses of Cu films are acquired. Then, the relationship line between the inductance difference and the LODC is also obtained and fitted through the MATLAB tool by using the linear least-squares fitting method and the fitted curves are presented in Fig. 12. When the thickness of Cu film gets thicker, the SOR is bigger. The SOR is

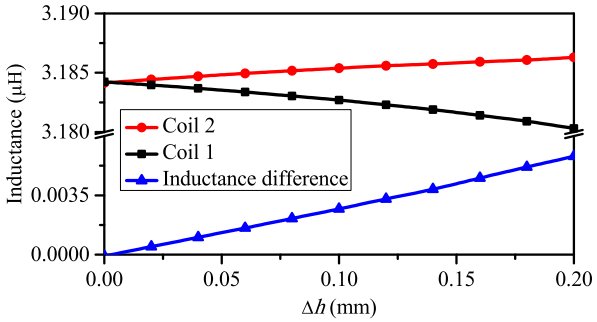

FIGURE 9. Inductances and inductance difference of two coils under different LODCs.

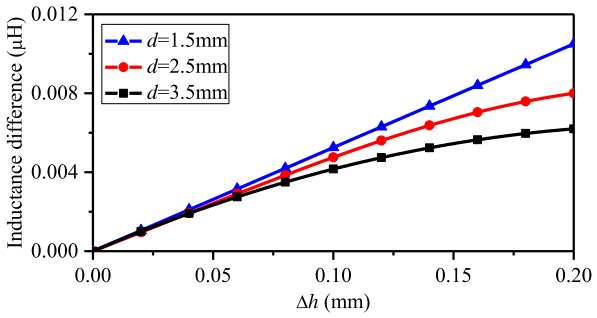

FIGURE 10. Inductance difference of two coils under different d and Δh.

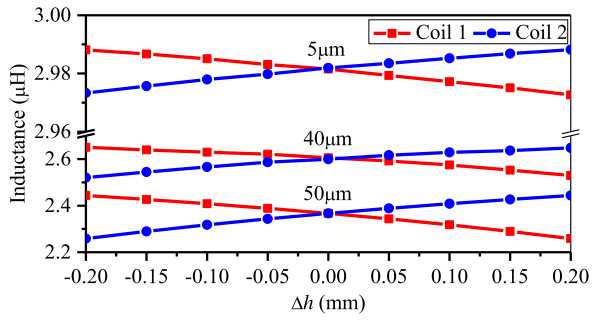

FIGURE 11. Inductances of two coils under different LODCs.

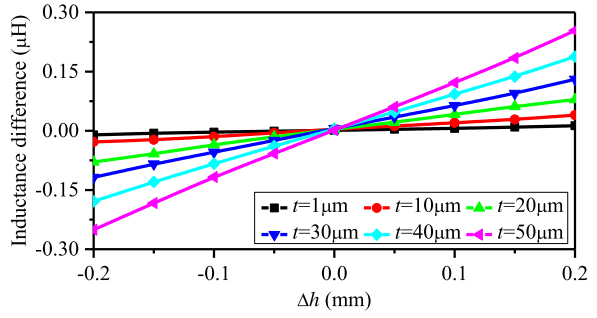

FIGURE 12. The relationship between inductance difference and LODC for different thicknesses of Cu films on silicon wafer.

proportional to the thickness of Cu film and has no relationship with the LODC. When the slope parameter is used to determine the thickness of Cu film, the variable LODC no longer posts a negative effect but an indispensable indicator of the thickness.

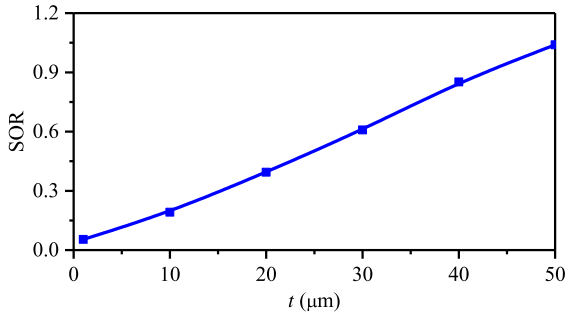

FIGURE 13. The relationship between SOR and thickness of Cu film on silicon wafer.

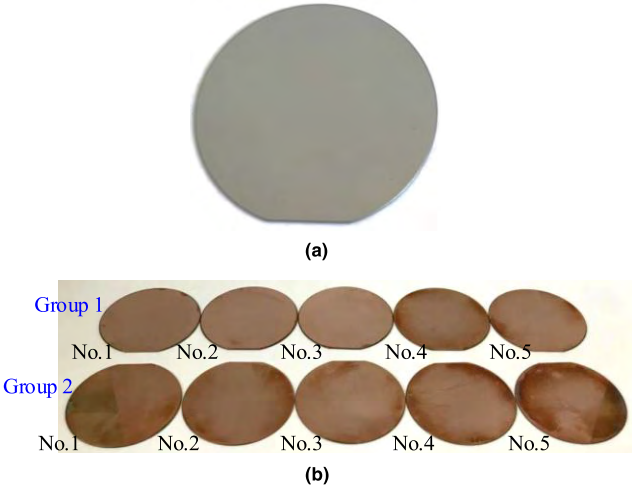

FIGURE 14. Silicon wafer specimens. (a) Silicon wafer without Cu film, (b) silicon wafers with different thicknesses of Cu film.

The thicknesses of Cu films and their corresponded simulated SOR values are acquired, fitted and displayed in Fig. 13. With the increase of the thickness of Cu film, the SOR value increases monotonically. Referring to Figs. 11–13, the LODC has no effect on the thickness of Cu film.

IV. EXPERIMENT AND DISCUSSION

To validate the theoretical analysis of the proposed method for the measurement of the thickness of Cu film on the silicon wafer, a double-coil sensor is fabricated and a test platform is built, and the experiment is implemented.

A. CU FILM ON SILICON WAFER PREPARATION

Different silicon wafers with different thicknesses of Cu film are prepared by using physical vapor deposition (PVD) method in the experiment. Fig. 14(a) shows a silicon wafer of 4 inches without Cu film. During the magnetron sputtering, the vacuum of the cavity is set as 1.5×10^{-3} Pa, the flow of the argon is 80 sccm, the voltage between counter electrodes is 850 V $\sim$ 900 V, and the diameters of the sputtering range and the targeted material are 60 mm and 62 mm, respectively.

TABLE 1. The Cu film thicknesses of specimens.

Specimen No.	1	2	3	4	5
Group 1 (nm)	151	240	305	368	447
Group 2 (nm)	105	165	213	278	340

The silicon basement is placed on the pallet with the rotation speed of 20 rpm, and the power of the PVD instrument is 150 W.

By adjusting the sputtering duration time, two groups of silicon wafers with different thicknesses of Cu films are obtained, termed as Group 1 and Group 2, as shown in Fig. 14(b). Each group consists of different silicon wafers with different thicknesses of Cu films ranging from 100 nm to 450 nm, numbered as 1 $\sim$ 5 in sequence. The average thicknesses of Cu films of specimens are further measured and confirmed by the 4PP method. The Cu film thicknesses of specimens are listed in detail in Table 1. Group 1 is used to calibrate the experiment setup and Group 2 is utilized for evaluating the error for the proposed measurement method.

Fig. 15 illustrates the precise thickness measurement for the Cu film on the silicon wafer. One fabricated silicon wafer with a Cu film of 305 nm thickness is placed on the 4PP instrument (Creative Design Engineering, ResMap 178) shown in Fig. 15(a), and the different measured values are obtained at measurement points along the measurement route (diameter line) as shown in Fig. 15(b). Then, the relationship between different measured values and measurement route is drawn and shown in Fig. 15(c). The precise thickness of Cu film on the silicon wafer is the average value of all measured values.

B. EXPERIMENT SETUP

Fig. 16 shows the photograph of the fabricated double-coil sensor which has two input ports and two output ports. The support is manufactured by the 3D printing for fixing the two coils and the auxiliary circuit. The measurement instruments used to implement the experiment are illustrated in Fig. 17. The function/arbitrary waveform generator (Rigol DG4162) provides the sinusoidal wave signal with a working frequency (e.g., 0.5 MHz) and amplitude of 10 Vpp, which is fed into the power amplifier and power divider (MHS5200P), and then is delivered to the double-coil sensor. The output signal from the double-coil sensor is amplified through the instrument amplifier (AD8222) and collected by the data acquisition (DAQ) card (Advantech Company, USB-4716, 200 KS/s). The XYZ positioning table is employed and controlled by the workstation. The double-coil sensor can be moved on z direction and x direction by a micro-meter step through two motors, respectively. The received data are processed by the workstation and the thickness of Cu film on the silicon wafer is obtained. Different modules are connected by the RF coaxial cables assembling BNC (50 Ω, Pomona Electronics Model 2249) and BNC-SMA converters.

The distance of two eddy current coils of the double-coil sensor is 2.8 mm, and the excitation signals fed into the

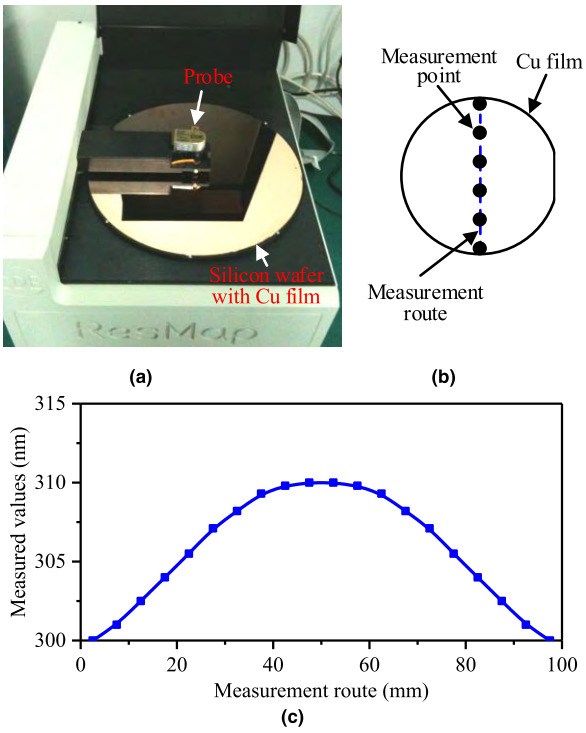

FIGURE 15. (a) 4PP instrument and silicon wafer with a Cu film of 305 nm thickness, (b) radius mode, and (c) the relationship between measured values and measurement route.

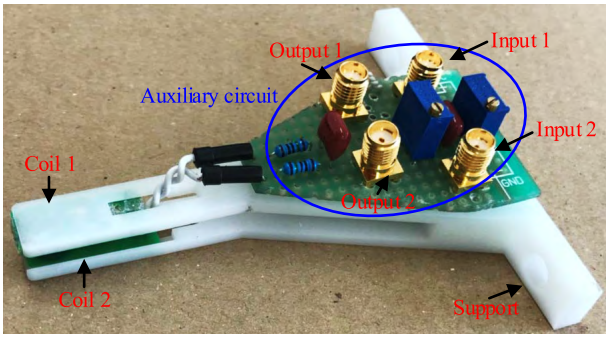

FIGURE 16. Photograph of fabricated double-coil sensor.

two coils are the same. Also, the silicon wafer specimens are held on the rotation stage by the vacuum chuck.

Two test modes based on the measurement route are taken: Radius mode and Globe mode. In the radius mode, only the thickness distribution data along the diameter direction of the silicon wafer are collected. It can utilize a few limited measured values to extract the average thickness of Cu film on the silicon wafer. In the globe mode, the double-coil sensor is moving along the x direction and the silicon wafer rotates along the axial direction simultaneously. The sensor can detect the Cu film thickness repeatedly from the center to the edge of the silicon wafer. Also, it real-timely supports the SFP machine to adjust the amount of electrolyte on the silicon wafer according to the thickness distribution and guarantees the uniformity of Cu film removal rate.

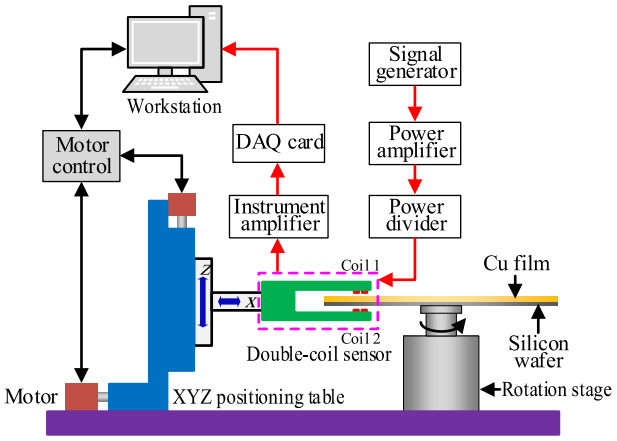

FIGURE 17. Block diagram of the experiment setup.

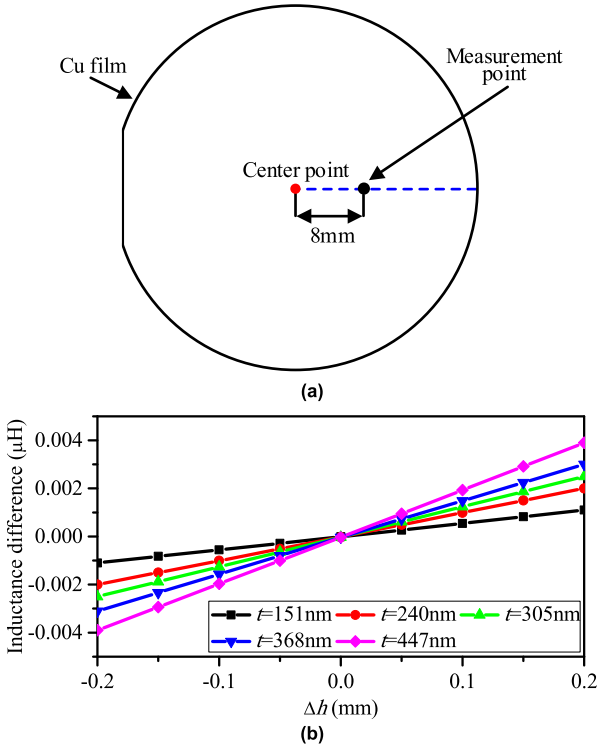

FIGURE 18. (a) Radius mode, and (b) inductance differences with different LODCs for specimens in Group 1.

C. MEASURED RESULTS AND DISCUSSION

The specimens in Group 1 are used to calibrate the experiment setup. During the experiment, the LOD (h) between the Cu film and the coil 1 is varying from 1.2 mm to 0.8 mm with a step of 0.05 mm, which means the LODC (Δh) is from -0.2 mm to 0.2 mm. The double-coil sensor is fixed and the two coaxial coils are located at the measurement point which is 8 mm away from the center point as shown in Fig. 18(a). Along the diameter direction of the silicon wafer, the average voltage of each coil-capacitor tank is measured and then the inductance of the coil is extracted. The relationship between the inductance difference of the two coils and LODC is analyzed and presented in Fig. 18(b).

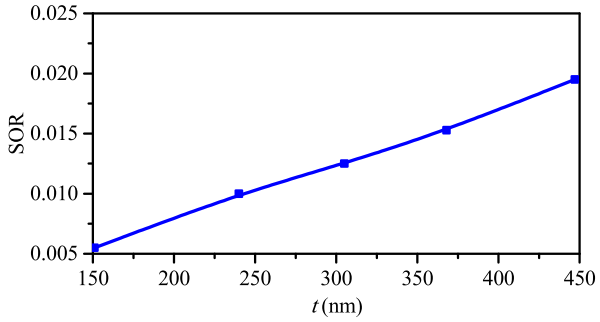

FIGURE 19. SOR under different thicknesses of Cu film for specimens of Group 1.

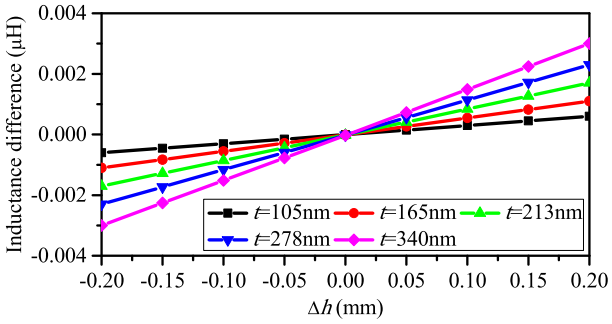

FIGURE 20. Inductance differences with different LODCs for specimens in Group 2.

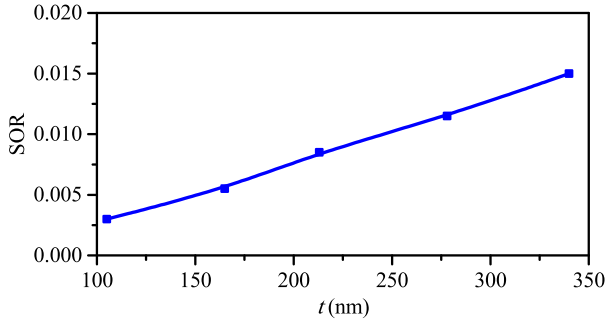

FIGURE 21. SOR under different thicknesses of Cu films for specimens in Group 2.

As the LODC increases, the inductance difference also increases. Furthermore, the SOR values respectively corresponding to the specimens in Group 1 are extracted and fitted by using the linear least-squares fitting method. The fitted curve is displayed in Fig. 19. When the thickness of Cu film increases, the SOR value also increases. The measured data show a good agreement with the simulated results as shown in Fig. 13.

The specimens in Group 2 is used to evaluate the accuracy of the proposed measurement method. The inductance differences with different LODCs for prepared specimens in Group 2 are collected and shown in Fig. 20. Then, the SOR values under different thicknesses of Cu films are extracted and displayed in Fig. 21.

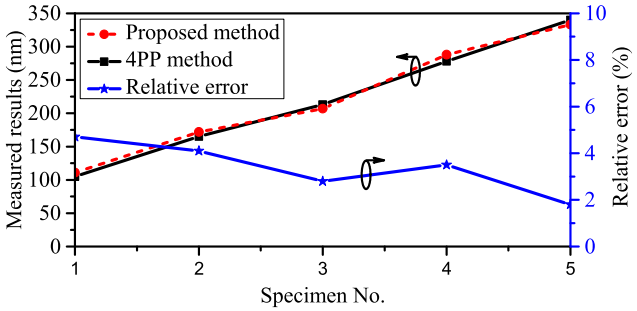

FIGURE 22. Comparison of different measurement methods and relative error.

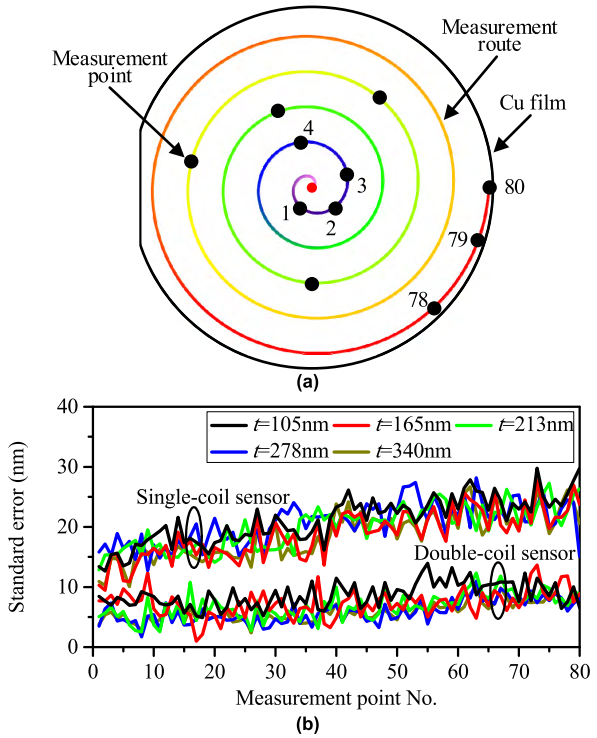

FIGURE 23. Globe mode measurement and error analysis. (a) Globe mode, (b) standard error.

As a comparison, the specimens in Group 2 are also measured by the 4PP method. Both measured results from the proposed measurement method and 4PP method are shown in Fig. 22, where they show a good agreement. The relative error δx is defined by

$$\delta x = |(x - x_0)/x_0| \times 100\% \tag{25}$$

where x is the measured value from the double-coil sensor and x_0 is the precise thickness of Cu film on the silicon wafer obtained by the 4PP method. The relative error is calculated and drawn in Fig. 22, and the maximum relative error is 4.7%, which satisfies the requirement in the SFP application.

D. ERROR ANALYSIS

Fig. 23(a) shows the measurement point distribution on the whole silicon wafer by using the global mode. By utilizing

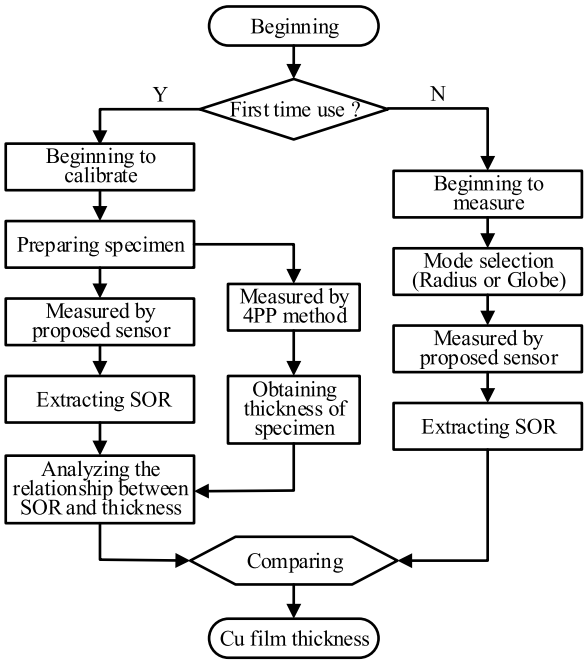

FIGURE 24. Measurement procedure flowchart on proposed noncontact measurement method based on double-coil sensor.

80 measurement points along the measurement route, the thickness profile on the silicon wafer is acquired. By the noncontact measurement method based on double-coil sensor, the data collection is repeatedly operated 10 times at every measurement point. Then, 800 measured values are processed by the formula of the standard error σ_0, which is defined as

$$\sigma_0 = \sqrt{\frac{1}{N}\sum_{i=1}^{N}(x_i - \mu)^2} \tag{26}$$

where N is the repeated measurement times at each measurement point, x_i is the measured value, and μ is the arithmetic mean of N measured values. For different specimens in Group 2, the standard errors are resolved and fitted at different measurement points, as shown in Fig. 23(b). It is found that the standard errors are between 2 nm and 13 nm. Similarly, the experiment is conducted by the measurement method based on a single coil, and the calculated standard errors are shown in Fig. 23(b), which vary from 10 nm to 30 nm. It is obvious that the standard errors increase with the measurement points moving toward the edge of the silicon wafer due to more runout position error at the edge of the silicon wafer. By comparison, the proposed noncontact measurement method based on double-coil sensor is more effective to eliminate the vibration effect of silicon basement and reduces the measurement error.

Referring to the above illustrations and experiments, the proposed measurement method procedure is summarized and presented in Fig. 24. Firstly, the measurement system based on double-coil sensor needs to be calibrated. A series of specimens with different thicknesses of Cu films on the

silicon wafer are prepared and then measured by both the 4PP method and proposed double-coil sensor. The relationship between SOR and thickness of Cu film is determined and saved as the reference data set. Then, the radius and globe modes can be selected, and the SOR is extracted. By comparison with the reference data, the thickness of Cu film can be obtained.

V. CONCLUSION

In this paper, a novel noncontact measurement method based on double-coil sensor has been investigated to measure the thickness of Cu film on the silicon wafer, which gives rise to the nondestructive and LODC-immune advantages for SFP application. Due to the linear inductance difference with LODC between two identical coaxial coils and Cu film, their relationship is extracted to confirm the thickness of Cu film on the silicon wafer, which rejects the disturbance of the LODC occurring in the measurement system by using a single coil. The interaction equivalent circuit model of Cu film and two coils of double-coil sensor is discussed as well as the coil design and its lumped parameter extraction are analyzed. Meantime, the electromagnetic field simulations are conducted to observe the distribution and intensity of the magnetic field under different Cu film thicknesses. Extensive experiments are implemented to demonstrate the theoretical analysis and feasibility of the proposed measurement method and further validate the capability for the submicron thickness measurement of Cu film which ranges from 100 nm to 500 nm. The maximum relative error of 4.7% and standard error ranging from 2 nm to 13 nm are got for prepared specimens. In the future, the spatial resolution will be improved and the proposed measurement system is further optimized to be applied in the SFP machine.

REFERENCES

[1] P. B. Zantye, A. Kumar, and A. K. Sikder, "Chemical mechanical planarization for microelectronics applications," *Mater. Sci. Eng., R, Rep.*, vol. 45, nos. 3–6, pp. 89–220, Oct. 2004.
[2] P. Wrschka, J. Hernandez, G. S. Oehrlein, and J. King, "Chemical mechanical planarization of copper damascene structures," *J. Electrochem. Soc.*, vol. 147, no. 2, pp. 706–712, 2000.
[3] D. Shamiryan, T. Abell, F. Lacopi, and K. Maex, "Low-k dielectric materials," *Mater. Today*, vol. 7, no. 1, pp. 34–39, Jan. 2004.
[4] J.-B. Chiu, C.-C. Yu, and S.-H. Shen, "Application of soft landing to the process control of chemical mechanical polishing," *Microelectron. Eng.*, vol. 65, no. 3, pp. 345–356, Mar. 2003.
[5] J. Pallinti, S. Lakshminarayanan, W. Barth, P. Wright, M. Lu, S. Reder, L. Kwak, W. Catabay, D. Wang, and F. Ho, "An overview of stress free polishing of Cu with ultra low-k (k<2.0) films," in *Proc. IEEE Int. Interconnect Techn. Conf.*, Burlingame, CA, USA, Jun. 2003, pp. 83–85.
[6] T. Kojima, M. Miyajima, F. Akaboshi, T. Yogo, S. Ishimoto, and A. Okuda, "Application of CMP process monitor to Cu polishing," *IEEE Trans. Semicond. Manuf.*, vol. 13, no. 3, pp. 293–299, Aug. 2000.
[7] H. Hocheng and Y.-L. Huang, "A comprehensive review of end point detection in chemical mechanical polishing for deep-submicron integrated circuits manufacturing," *Int. J. Mater. Product Technol.*, vol. 18, nos. 4–6, pp. 469–486, 2003.
[8] T. Bibby and K. Holland, "Endpoint detection for CMP," *J. Electron. Mater.*, vol. 27, no. 10, pp. 1073–1081, 1998.
[9] Z. Qu, Q. Zhao, Y. Meng, T. Wang, D. Zhao, Y. Men, and X. Lu, "*In-situ* measurement of Cu film thickness during the CMP process by using eddy current method alone," *Microelectron. Eng.*, vol. 108, pp. 66–70, Aug. 2013.
[10] D. Windover, E. Barnet, J. Summers, C. Gribbin, T. M. Lu, A. Kumar, H. Bakhru, and S. L. Lee, "Development of an in-line X-ray reflectivity technique for metal film thickness measurement," in *Proc. AIP Conf.*, vol. 550, Mar. 2001, pp. 243–248.
[11] N. Bowler and Y. Q. Huang, "Electrical conductivity measurement of metal plates using broadband eddy-current and four-point methods," *Meas. Sci. Technol.*, vol. 16, no. 11, pp. 2193–2200, 2005.
[12] W. Li, H. Wang, and Z. Feng, "Non-contact online thickness measurement system for metal films based on eddy current sensing with distance tracking technique," *Rev. Sci. Instrum.*, vol. 87, no. 4, pp. 045005-1–045005-9, Apr. 2016.
[13] H. Wang, W. Li, and Z. Feng, "Noncontact thickness measurement of metal films using eddy-current sensors immune to distance variation," *IEEE Trans. Instrum. Meas.*, vol. 64, no. 9, pp. 2557–2564, Sep. 2015.
[14] W. Li, Y. Ye, K. Zhang, and Z. Feng, "A thickness measurement system for metal films based on eddy-current method with phase detection," *IEEE Trans. Ind. Electron.*, vol. 64, no. 5, pp. 3940–3949, May 2017.
[15] F. Sakran, M. Golosovsky, H. Goldberger, D. Davidov, and A. Frenkel, "High-frequency eddy-current technique for thickness measurement of micron-thick conducting layers," *Appl. Phys. Lett.*, vol. 78, no. 11, pp. 1634–1636, Jan. 2001.
[16] Y. Danon, C. Lee, C. Mulligan, and G. Vigilante, "Characterizing tantalum sputtered coatings on steel by using eddy currents," *IEEE Trans. Magn.*, vol. 40, no. 4, pp. 1826–1832, Jul. 2004.
[17] W. Yin and A. J. Peyton, "Thickness measurement of metallic plates with an electromagnetic sensor using phase signature analysis," *IEEE Trans. Instrum. Meas.*, vol. 57, no. 8, pp. 1803–1807, Aug. 2008.
[18] W. Yin, A. J. Peyton, and S. J. Dickinson, "Simultaneous measurement of distance and thickness of a thin metal plate with an electromagnetic sensor using a simplified model," *IEEE Trans. Instrum. Meas.*, vol. 53, no. 4, pp. 1335–1338, Aug. 2004.
[19] W. Yin and K. Xu, "A novel triple-coil electromagnetic sensor for thickness measurement immune to lift-off variations," *IEEE Trans. Instrum. Meas.*, vol. 65, no. 1, pp. 164–169, Jan. 2016.
[20] M. Fan, B. Cao, G. Tian, B. Ye, and W. Li, "Thickness measurement using liftoff point of intersection in pulsed eddy current responses for elimination of liftoff effect," *Sens. Actuators A, Phys.*, vol. 251, pp. 66–74, Nov. 2016.
[21] W. Yin and A. J. Peyton, "Thickness measurement of non-magnetic plates using multi-frequency eddy current sensors," *NDT E Int.*, vol. 40, no. 1, pp. 43–48, Jan. 2007.
[22] G. Y. Tian and A. Sophian, "Reduction of lift-off effects for pulsed eddy current NDT," *NDT E Int.*, vol. 38, no. 4, pp. 319–324, 2005.
[23] Y. Yu, Y. Yan, F. Wang, G. Tian, and D. Zhang, "An approach to reduce lift-off noise in pulsed eddy current nondestructive technology," *NDT E Int.*, vol. 63, pp. 1–6, Apr. 2014.
[24] G. Y. Tian, Y. Li, and C. Mandache, "Study of lift-off invariance for pulsed eddy-current signals," *IEEE Trans. Magn.*, vol. 45, no. 1, pp. 184–191, Jan. 2009.
[25] Z. Qu, Q. Zhao, and Y. Meng, "Improvement of sensitivity of eddy current sensors for nano-scale thickness measurement of Cu films," *NDT E Int.*, vol. 61, pp. 53–57, Jan. 2014.
[26] D. Mayer and B. Ulrych, "Complex inductance and its computer modelling," *J. Elect. Eng.*, vol. 53, nos. 1–2, pp. 24–29, 2002.
[27] G. Kim and B. Lee, "Alternative expressions for mutual inductance and coupling coefficient applied in wireless power transfer," *J. Electromagn. Eng. Sci.*, vol. 16, no. 2, pp. 112–118, Apr. 2016.
[28] J. Gilchrist and E. H. Brandt, "Screening effect of Ohmic and superconducting planar thin films," *Phys. Rev. B, Condens. Matter*, vol. 54, no. 5, pp. 3530–3544, Aug. 1996.
[29] W. Wang, Y. Chen, S. Yang, A. Chan, Y. Wang, and Q. Cao, "Design and experiment of wireless power transfer systems via electromagnetic field near-zone region," *Int. J. Electron.*, vol. 103, no. 10, pp. 1736–1747, Feb. 2016.
[30] W. Wang, Y. Chen, S. Yang, X. Zheng, and Q. Cao, "Design of a broadband electromagnetic wave absorber using a metamaterial technology," *J. Electromagn. Waves*, vol. 29, no. 15, pp. 2080–2091, Sep. 2015.

ZILIAN QU received the Ph.D. degree in mechanical engineering from Tsinghua University, Beijing, China, in 2014. From 2014 to 2016, he was a Postdoctoral Research Associate with the Tsinghua University, China. From 2016 to 2017, he was a Research Fellow with Nanyang Technological University, Singapore. He is currently an Assistant Professor with the Beijing Information Technology College, China. His current research interests include non-destructive testing and evaluation, design of electromagnetic sensor, and manufacturing technology of integrated circuit.

He is a senior member of Chinese Mechanical Engineering Society (CMES).

WENSONG WANG (M'18) received the Ph.D. degree from the Nanjing University of Aeronautics and Astronautics, Nanjing, China, in 2016. From 2013 to 2015, he was a Visiting Scholar with the University of South Carolina, Columbia, USA. In 2017, he joined Nanyang Technological University, Singapore, as a Research Fellow. His current research interests include RF/microwave components and systems, inter/intra-chip wireless interconnect, power wireless transfer, signal integrity, and rail non-destructive real-time monitoring.

SHUHUI YANG (M'13) received the B.Sc. degree from Zhejiang University, Hangzhou, China, in 1994, the M.Sc. degree from Communication University of China, Beijing, China, in 2000, and the Ph.D. degree from the Institute of Microelectronics of the Chinese Academy of Sciences, Beijing, China, in 2003.

From 2003 to 2015, he was with Beijing Information and Science and Technology University as a Professor. In 2015, he joined Communication University of China, and currently as a Professor and Director of the Department of Communication Engineering. In 2008, he was a Visiting Scholar and an Adjunct Associate Professor with the University of South Carolina (USC), Columbia, USA. In 2011, he was a Visiting Scholar with Victoria University, Melbourne, Australia. From 2013 to 2014, he was a Visiting Professor with USC. He is the senior member of the Chinese Institute of Electronics (CIE). His current research interests include the electromagnetic metamaterials, passive microwave components, electromagnetic compatibility (EMC), signal integrity (SI), and wireless inter/intra-chip communication system.

QUQIN SUN received the B.Sc. and Ph.D. degrees from Huazhong University of Science and Technology, Wuhan, China, in 2011 and 2016, respectively. He was a Research Associate with the Institute of Fluid Physics of China Academy of Engineering Physics till 2018 and currently is a Research Fellow of Nanyang Technological University, Singapore. His current research interests include electromangetic coil design, machine learning, and nondestructive testing of complex structures under extreme environments.

ZHONGYUAN FANG received the B.Sc. degree in microelectronics from Fudan University, in 2016. He is currently pursuing the Ph.D. degree with full scholarship with the Electrical and Electronic Engineering Department, Nanyang Technological University, Singapore. From 2014 to 2016, he was an undergraduate Research Assistant with the State Key Laboratory of ASIC and System, Shanghai. Since 2016, he has been with the Virtus IC Design Center of Excellence, Singapore. His research interests include analog/mixed signal and low-power integrated circuit design, energy-efficient algorithms for physiological signal extraction, AI-enabled IC design, and RF/wireless communication circuits and systems design and testing for biomedical applications. He received the Excellent Student Scholarship from Fudan University, in 2016. He is also a recipient of the Fudan Science and Technology Innovation Award. He received the highest grade on his B.Sc. graduation thesis. His work has been published in ISSCC, ISCAS, TCAS-I, etc.

YUANJIN ZHENG (SM'06) received the B.Eng. and M.Eng. degrees from Xi'an Jiaotong University, Xi'an, China, in 1993 and 1996, respectively, and the Ph.D. degree from Nanyang Technological University, Singapore, in 2001.

From July 1996 to April 1998, he was with the National Key Laboratory of Optical Communication Technology, University of Electronic Science and Technology of China. In 2001, he joined the Institute of Microelectronics (IME), Agency for Science, Technology, and Research (A*STAR), and had been a Principle Investigator and Group Leader. In July 2009, he joined the Nanyang Technological University, and currently as an Associate Professor and a Program Director. He has authored or coauthored over 300 international journals and conference papers, 22 patents filed, and 5 book chapters. He has led and completed projects by working with industry partners and developing commercial products. His research interests include integrated circuits design, 3D imaging and display, and SAW/BAW/MEMS sensors for NDT, etc.